scientific reports

Check for updates

OPEN

Network pharmacology, prognostic analysis and experimental validation elucidate the therapeutic mechanism of Dingxiang Guanshitong in esophageal cancer

Hao Zhang[1], Shi-qi Wang[2], Xiao-qi Chen[2], Li-qi Li[1], Yu-hong Zheng[1], Ya-ling Zhang[2], Xue-wen Diao[3], Pei-yu Yan[1,4]✉ & Yu-ling Zheng[2]✉

This study aimed to investigate the target genes of active components in Dingxiang Guanshitong (DGST) and evaluate their significance in the prognosis of esophageal cancer (EC) through integrated approaches, including network pharmacology, molecular docking, prognostic analysis, and in vitro experiments. EC-related data were obtained from TCGA database, while SymMap and TCMSP databases were utilized to identify DGST's bioactive components and their targets. A comprehensive network was constructed to map component-target-pathway interactions. Bioinformatics analysis revealed 113 key signaling pathways and 424 differentially expressed targets associated with DGST and EC. Univariate Cox regression analysis identified 21 target genes significantly correlated with overall survival (OS) in EC patients, among which six exhibited pharmacological activity. Molecular docking confirmed strong binding affinities between DGST's active components and critical targets. In vitro experiments demonstrated that DGST suppressed migration, invasion, and proliferation of TE-1 and EC-109 cell lines while promoting apoptosis. Furthermore, DGST significantly upregulated the protein and mRNA expression of the prognostic factor NFKBIA, while downregulating GPER1, HK2, MAOB, TNFRSF10B, and ECE1. This study is the first to elucidate the molecular mechanisms underlying DGST's anti-EC effects. DGST exerts its anti-cancer activity by targeting prognosis-related genes and modulating the expression of critical molecular markers, thereby inhibiting EC progression and improving therapeutic outcomes. These findings provide a robust scientific foundation for the clinical application of DGST and further exploration of its mechanistic basis.

Keywords Dingxiang guanshitong, Prognostic target genes, Esophageal cancer, Network pharmacology, Molecular docking, Pathway enrichment

Abbreviations

DGST	Dingxiang guanshitong
EC	Esophageal cancer
GO	Gene ontology
MF	Molecular function
KEGG	Kyoto encyclopedia of genes and genomes
TCMSP	Traditional chinese medicine systems pharmacology database and analysis platform
UHPLC-MS/MS	Ultra-high-performance liquid chromatography-tandem mass spectrometry
RT	Retention time
MAOB	Monoamine oxidase B
NFKBIA	Nuclear factor of kappa light polypeptide gene enhancer in B-Cells inhibitor, alpha
TNFRSF10B	Tumor necrosis factor receptor superfamily member 10B

[1]Faculty of Chinese Medicine, Macau University of Science and Technology, SAR, Macao, China. [2]The First Affiliated Hospital of Henan University of Chinese Medicine, Zhengzhou, China. [3]Henan University of Traditional Chinese Medicine, Zhengzhou, China. [4]State Key Laboratory of Quality Research in Chinese Medicines, Macau University of Science and Technology, Macao, Macao SAR, China. ✉email: pyyan@must.edu.mo; zhengyl@hactcm.edu.cn

ECE1	Endothelin converting enzyme 1
HK2	Hexokinase 2
GPER1	G protein-coupled estrogen receptor 1

Esophageal cancer (EC) is a highly aggressive malignancy and the sixth leading cause of cancer-related deaths globally[1]. Approximately 85% of EC cases are esophageal squamous cell carcinoma, with China reporting some of the highest incidence and mortality rates worldwide[2]. Late diagnosis and high metastasis rate pose significant challenges to treatment[3,4]. Current therapies, including surgery, radiotherapy, and chemotherapy, have limited efficacy and are often associated with severe adverse effects[5–7]. Traditional Chinese medicine (TCM), recognized for its multi-faceted mechanisms, reduced side effects, and therapeutic potential, offers a promising complementary approach in cancer treatment[8–10].

Dingxiang Guanshitong (DGST), patented under CN202011047671.5, is a formulation developed by renowned TCM expert Dr. Zheng Yuling based on her extensive clinical experience. Currently utilized as an in-hospital preparation at Henan Provincial Hospital of Traditional Chinese Medicine, DGST comprises nine medicinal herbs: *Syzygium aromaticum* (L.) Merr. & L.M.Perry (Ding Xiang, DX), *Aquilaria malaccensis* Lam. (Chen Xiang, CX), *Panax ginseng* C.A.Mey. (Ren Shen, RS), *Rehmannia glutinosa* (Gaertn.) DC. (Di Huang, DH), *Cinnamomum verum* J.Presl (Rou Gui, RG), *Asarum sieboldii* Miq. (Xi Xin, XX), *Curcuma longa* L. (Jiang Huang, JH), *Panax notoginseng* (Burkill) F.H.Chen (San Qi, SQ), and *Sargassum*C. Agardh (Hai Zao, HZ). Clinical studies have shown that DGST alleviates symptoms, improves quality of life, and enhances survival rates in patients with EC[11]. However, the precise mechanisms and bioactive components underlying its therapeutic effects remain unclear, warranting further investigation.

Network pharmacology offers a robust framework for elucidating the mechanisms of TCM by integrating drug components, targets, and pathways within complex disease-gene networks. This approach enables a multidimensional analysis of TCM formulations, revealing their therapeutic potential[12]. Unlike reductionist methods that focus on single targets, network pharmacology aligns well with TCM's holistic philosophy, enabling systematic analysis of TCM formulations and their therapeutic effects. This study employs network pharmacology, molecular docking, and prognostic analysis to identify key active components and therapeutic targets of DGST in EC, evaluate its prognostic significance, and validate findings through in vitro experiments, offering a comprehensive foundation for its application in EC therapy.

Methods

Network pharmacology study of DGST in the treatment of EC

Construction and analysis of the network of active components and target genes of DGST

The mRNA expression profiles and sample data of EC tumor samples were obtained from https://xenabrowser.net/datapages/. Expression profile datasets containing survival information were selected for further analysis. The nine herbal ingredients of DGST—clove, agarwood, ginseng, rehmannia, cinnamon, asarum, turmeric, notoginseng, and seaweed—were retrieved from the Symmap database (http://www.symmap.org/search/) to identify their chemical components and targets. Active components were filtered based on oral bioavailability (OB ≥ 20%), a widely accepted threshold for evaluating pharmacological properties. Similarly, key targets were selected using a significance threshold of p-value < 0.05. The relationship between DGST's active components and target genes was further analyzed using the TCMSP database (https://tcmsp-e.com/tcmsp.php).

Data underwent log2-transformation and quantile normalization to ensure consistency. Probes were mapped to genes, and redundant or empty probes were excluded. For genes with multiple probes, median expression values were used. The integrated dataset of active components, targets, and EC-related genes was visualized as an interaction network using Cytoscape v3.9.1.

Differential gene expression and pathway enrichment analysis in EC

Differentially expressed genes (DEGs) in patients with EC were identified using the 'limma' R package. Genes were filtered using a significance threshold of p-value < 0.05 to distinguish between disease and control groups. GO functional enrichment analysis, and Kyoto Encyclopedia of Genes and Genomes (KEGG) pathway analysis were performed on the DEGs using the clusterProfiler R package, offering insights into molecular functions and biological pathways.

Differential target genes of DGST

DGST differential target genes were identified by intersecting DGST-associated target genes with EC-specific DEGs. Protein-protein interaction (PPI) data were retrieved from the STRING database (https://string-db.org/) to construct a PPI network, which was visualized using Cytoscape v3.9.1. The MCODE plugin was employed to detect significant modules within the network.

Identification of key pathways

KEGG pathway analysis was conducted on DGST's differential target genes using the clusterProfiler R package to identify potential therapeutic pathways. KEGG's extensive database facilitates an in-depth understanding of genome-level metabolic pathways and biological systems[13,14].

Molecular docking

Molecular docking is a computational technique used to analyze the interactions between small molecules and their target sites through structural modeling. By simulating molecular binding processes, it identifies binding sites, evaluates binding affinity, and provides critical insights for drug design and optimization.

This study conducted molecular docking analysis on key target genes identified through network pharmacology and their associated active components in DGST. Chemical structure files of DGST's active components were retrieved from the TCMSP database, while three-dimensional structure files of target gene proteins were obtained from the PDB database. Docking was conducted using the online software deepmice, generating PSE files. Binding conformations were visualized using PyMOL to evaluate molecular interactions.

Prognostic analysis of key markers

Univariate Cox regression analysis was performed to identify target genes associated with DGST pathways. The Benjamini & Hochberg method was applied to adjust P-values, controlling the false discovery rate in multiple hypothesis testing. EC samples were categorized into high-expression and low-expression groups based on the median expression levels of these genes. Prognostic analysis was conducted using the Survival R package to evaluate correlations between gene expression and patient outcomes.

Study of DGST chemical composition

Preparation of the drug

Herbal materials were mixed and soaked in 10 times their volume of water for 30 min before being boiled at 100 °C for 40 min. The decoction was filtered through gauze, and the herbs were boiled again under identical conditions. The two decoctions were combined and concentrated to a final solution with a concentration of 1.1 g/mL. All herbal materials were sourced from the First Affiliated Hospital of Henan University of Chinese Medicine (Zhengzhou, China).

Chromatography and mass spectrometry methods

Samples were thawed and mixed thoroughly by vortexing. A 200 µL aliquot of each sample was mixed with an internal standard-containing 70% methanol extraction solution in a centrifuge tube. After vortexing and centrifugation for 15 min, the supernatant was collected, filtered, and transferred to sample vials. Analyses were conducted using the UPLC-ESI-MS/MS system with a tandem mass spectrometry setup. Data were processed using Analyst 1.6.3 software, and compound structure identification was performed by Wuhan MetWare Biotechnology Co., Ltd.

In-vitro validation

Key reagents

RPMI-1640 medium, foetal bovine serum (FBS), and trypsin digestion solution were obtained from Solarbio (China). Foetal bovine serum was sourced from ExCell Bio (China). Cell culture flasks and dishes were purchased from Corning Costar (USA). The CCK-8 kit was acquired from Glpbio (USA), while the Annexin V-FITC/PI Apoptosis Kit was purchased from Elabscience (China). Antibodies against *MAOB* (GTX105970), IκBα (GTX110521), GPR30 (GTX107748), *HK2* (GTX111525), and Tubulin (GTX628820) were procured from Genetex (USA). Antibodies against *ECE1* (YN2159) and DR5 (TT7791 were obtained from Immunoway (China). HRP-conjugated goat anti-rabbit secondary antibody (SA00001-2) and HRP-conjugated goat anti-mouse secondary antibody (SA00001-1) were sourced from Wuhan Sanying (China).

Preparation of drug-containing serum

Thirty healthy adult Sprague-Dawley (SD) rats, aged 56–70 days and weighing 200–250 g (License No.: SCXK2019-0008, Beijing Huafukang Bioscience Co., Ltd.), were used. All animals were housed in the SPF-grade Experimental Animal Center of the Henan University of Chinese Medicine. The rats were randomly divided into a control group and a DGST group, with 15 rats in each. The clinical DGST dose for adults is 106 g/60 kg, and the gavage dose for rats was calculated as 6.25 times the clinical dose based on body surface area. Rats in the DGST group received 11.04 g/kg DGST via gavage, while the control group received an equivalent volume of distilled water. Treatments were administered twice daily for 7 consecutive days. Serum samples were collected 1 h after the final administration, inactivated, sterilized by filtration, aliquoted, and stored at − 80 °C for future use. The animal experiments were approved by the Animal Ethics Committee of Henan University of Traditional Chinese Medicine (approval number: (IACUC-202302040). All experimental procedures strictly adhered to international and national animal welfare guidelines and regulations, as well as the ARRIVE guidelines.

Cell culture and grouping

TE-1 cells (Fuheng Biology, Shanghai, China) and EC-109 cells (The China Center for Type Culture Collection, Wuhan University, China) were cultured in RPMI-1640 medium supplemented with 10% FBS and 1% antibiotics, maintaining a pH of 7.2–7.4. Cells were incubated under standard conditions of 37 °C, 5% CO_2, and 95% humidity. Passaging was performed when cell confluency reached 70–90%. Both cell lines were divided into five groups: a control group (cultured in standard medium) and four experimental groups (cultured in medium containing 2, 5, 10, or 20% DGST-treated serum).

CCK-8 cell proliferation assay

After the cells were plated and incubated overnight, the original culture medium was discarded and replaced with 1640 culture medium without fetal bovine serum. The cells were cultured in an incubator set to 5% CO_2 at 37 °C for 24, 48, and 72 h. Wells containing only culture medium without cells were used as controls, and a blank control group without cells was also established. The original culture medium was then discarded, and 100 µL of 1640 culture medium containing 10% CCK-8 was added to each well. The cells were incubated at 37 °C for 1 h, and the absorbance of each well was measured at 450 nm using a microplate reader.

Cell apoptosis assay
Based on the optimal inhibition time determined from the CCK-8 assay, the optimal concentration of drug-containing serum was selected for this experiment. TE-1 and EC-109 cells in good growth condition were seeded evenly into six-well plates at a density of 5×10^6 cells per well. Drug-containing serum was added after 24 h of incubation in a CO_2 incubator. Following 48 h of incubation, cells were harvested and stained using the Annexin V-APC/7-AAD dual staining kit. Flow cytometry was performed to analyze the stained samples. Following 48 h of incubation, cells were harvested and stained using the Annexin V-APC/7-AAD dual staining kit. Flow cytometry was performed to analyze the stained samples.

Cell migration and invasion assay
Migration and invasion assays were conducted using a six-well Transwell system (Corning, Manassas, VA, USA). For the migration assay, 100 µL of cell suspension was added to the upper chamber, while 500 µL of medium containing 20% FBS was added to the lower chamber. The cells were incubated at 37 °C for 24 h in a humidified atmosphere with 5% CO_2. After incubation, the membranes were washed twice with PBS, fixed with 4% glutaraldehyde for 15 min, and stained with 0.1% crystal violet for 20 min. The membranes were then washed twice with PBS, and residual cells on the upper surface were removed with a cotton swab. Migrated cells were examined and counted under an inverted microscope in five randomly selected fields of view (×200 magnification).

For the invasion assay, the Transwell inserts were pre-coated with Matrigel (Corning, Manassas, VA, USA) at 100 µL per insert and allowed to polymerize for 1 h at 37 °C before cell seeding. The subsequent steps were performed as described for the migration assay.

Western blot analysis
Cells were harvested and lysed using RIPA lysis buffer (Solarbio, Beijing, China) to extract total protein from TE-1 and EC-109 cells. Protein concentrations were measured using a BCA assay kit (Solarbio, Beijing, China). Proteins were separated via sodium dodecyl sulfate-polyacrylamide gel electrophoresis (Epizyme, Shanghai, China) and transferred onto membranes using a wet blotting method. Membranes were incubated overnight at 4 °C with primary antibodies against MAOB, NFKBIA, GPER1, HK2, ECE1, TNFRSF10B, and tubulin. After incubation with secondary antibodies for 2 h at room temperature, proteins were detected using ECL chemiluminescent substrate (Solarbio, Beijing) and visualized using an imaging system.

Real-time quantitative polymerase chain reaction
Total RNA was extracted using TRIzol reagent (ThermoFisher), and cDNA synthesis was performed using a reverse transcription kit (TOYOBO). Real-time quantitative polymerase chain reaction (qPCR) was conducted with specific primers to quantify mRNA expression levels of key prognostic factors. Tubulin was used as the internal control gene, and data were analyzed using the $2^{-\Delta\Delta Ct}$ method. The sequences of primers used in this study are provided in Table 1.

Statistical analysis
For comparisons between two groups, normality was assessed first, followed by an independent sample t-test. For multiple group comparisons, normality and homogeneity of variance were tested before performing a one-way analysis of variance (ANOVA), followed by Newman–Keuls post hoc analysis. Results are expressed as the mean ± standard error of the mean, with a p-value < 0.05 considered statistically significant. Statistical analyses were conducted using SPSS 26, ImageJ, FlowJo, and GraphPad Prism 9.0.0 software.

Primer Name	Sequence	Gene ID	Length (bp)
hMAOB-F	GGAGCTAGGATTGGAGACCTAC	4129	83
hMAOB-R	CCCTGAAGGGGTATGATTTGC		
hECE1-F	GGGCATCCAGTACCAGACAAG	1889	132
hECE1-R	CCACAGGCGTAGCTGAAGAA		
hHK2-F	TGCCACCAGACTAAACTAGACG	3099	227
hHK2-R	CCCGTGCCCACAATGAGAC		
hNFKBIA-F	CTCCGAGACTTTCGAGGAAATAC	4792	135
hNFKBIA-R	GCCATTGTAGTTGGTAGCCTTCA		
hTNFRSF10B-F	ATGGAACAACGGGGACAGAAC	8795	195
hTNFRSF10B-R	CTGCTGGGGAGCTAGGTCT		
hGPER1-F	CACCAGCAGTACGTGATCGG	2852	120
hGPER1-R	CATCTTCTCGCGGAAGCTGAT		
htubulin-F	GGCCAAGGGTCACTACACG	10,381	85
htubulin-R	GCAGTCGCAGTTTTCACACTC		

Table 1. Primer sequences used for analyzing key prognostic factors associated with DGST.

Results

Network pharmacology analysis results

Identification of DGST active components

Using the SymMap database, 887 active components were identified from the nine medicinal herbs in DGST—clove, agarwood, ginseng, rehmannia, cinnamon, asarum, turmeric, notoginseng, and seaweed—based on the criterion of OB ≥ 20%. High oral bioavailability is typically regarded as a key indicator for evaluating the drug-like properties of bioactive molecules. Substances with OB ≥ 20% are considered to have high oral bioavailability. Additionally, 2,124 target genes were identified using a p-value < 0.05 (Supplementary File 1). The TCMSP database yielded 4,780 relationships between active components and target genes, of which 2,833 were deemed effective (Table 2), with complete data provided in Supplementary File 2.

Herb-active component-target network

Based on the nine medicinal herbs in DGST, 887 active components, 2,124 target genes, and 4,780 interactions (2,833 effective) between active components and potential target genes were identified. As shown in Fig. 1, these data were used to construct a network linking herbs, active components, and target genes. The results highlight quercetin (MOL000098) and acetic acid (MOL004480) as having the highest number of target genes, suggesting their potential as key active components. Active components are labeled with their MOL_IDs in Fig. 1, and detailed relationships are provided in Supplementary File 3.

3.1.3 Differential expression analysis and functional enrichment

Differential expression analysis was conducted using the limma package in R with a significance threshold of p-value < 0.05 to investigate differences in gene expression profiles between tumor samples from patients with EC and normal samples. A total of 3,924 differentially expressed genes were identified, comprising 810 upregulated genes and 3,114 downregulated genes (Fig. 2A, Supplementary File 4). Functional enrichment analysis was performed using the clusterProfiler package to evaluate the biological significance of these genes and explore their roles within and outside the cell. The analysis indicated that differentially expressed genes were primarily enriched in functions related to ATP activity, transcriptional regulation, and DNA repair (Fig. 2B, Supplementary File 5A). KEGG pathway analysis revealed that these genes were predominantly involved in the cell cycle, DNA replication, and the TP53 signaling pathway (Fig. 2C, Additional File 5B).

Differential target genes affected by DGST

The intersection of DEGs and DGST target genes identified 424 differential target genes affected by DGST (Supplementary File 6_DTG). To investigate the interactions among these genes, a PPI network was constructed using the STRING database. The PPI network was visualized with Cytoscape v3.9.1, and key modules were identified using the MCODE plugin. As shown in Fig. 3, analysis of the submodules highlighted genes such as MAOB and MSR1 as critical among the differentially expressed target genes.

Key pathways affected by DGST

To investigate the key pathways affected by DGST, molecular function prediction, and KEGG pathway analysis were conducted on the 424 differential target genes using the clusterProfiler package. The top 20 pathways, ranked by p-value, are provided in Fig. 4A and B, along with detailed results in Supplementary File 7A and 7B. Additionally, the relationships between molecules and pathways for genes with drug-related pairs in the TCMSP database are illustrated in Fig. 4C.

Herb	MOL_ID	Molecule_name	Target_name
Dingxiang	MOL010123	ZINC00394787	Cathepsin d
Dingxiang	MOL010123	ZINC00394787	Cholinesterase
Dingxiang	MOL010123	ZINC00394787	Cholinesterase
Dingxiang	MOL010123	ZINC00394787	Glycine amidinotransferase, mitochondrial
Dingxiang	MOL010557	WLN: 2OVR	Prostaglandin g/h synthase 1
Dingxiang	MOL010557	WLN: 2OVR	Muscarinic acetylcholine receptor m1
Dingxiang	MOL010557	WLN: 2OVR	Prostaglandin g/h synthase 2
Dingxiang	MOL010557	WLN: 2OVR	Sodium-dependent noradrenaline transporter
Dingxiang	MOL010557	WLN: 2OVR	Alpha 1a adrenergic receptor
Dingxiang	MOL010557	WLN: 2OVR	Sodium-dependent dopamine transporter
Dingxiang	MOL010557	WLN: 2OVR	Beta 2 adrenergic receptor
Dingxiang	MOL010557	WLN: 2OVR	Amine oxidase [flavin containing] b
Dingxiang	MOL010557	WLN: 2OVR	Amine oxidase [flavin containing] a

Table 2. Correspondence between DGST active components and their target genes, identified through network Pharmacology.

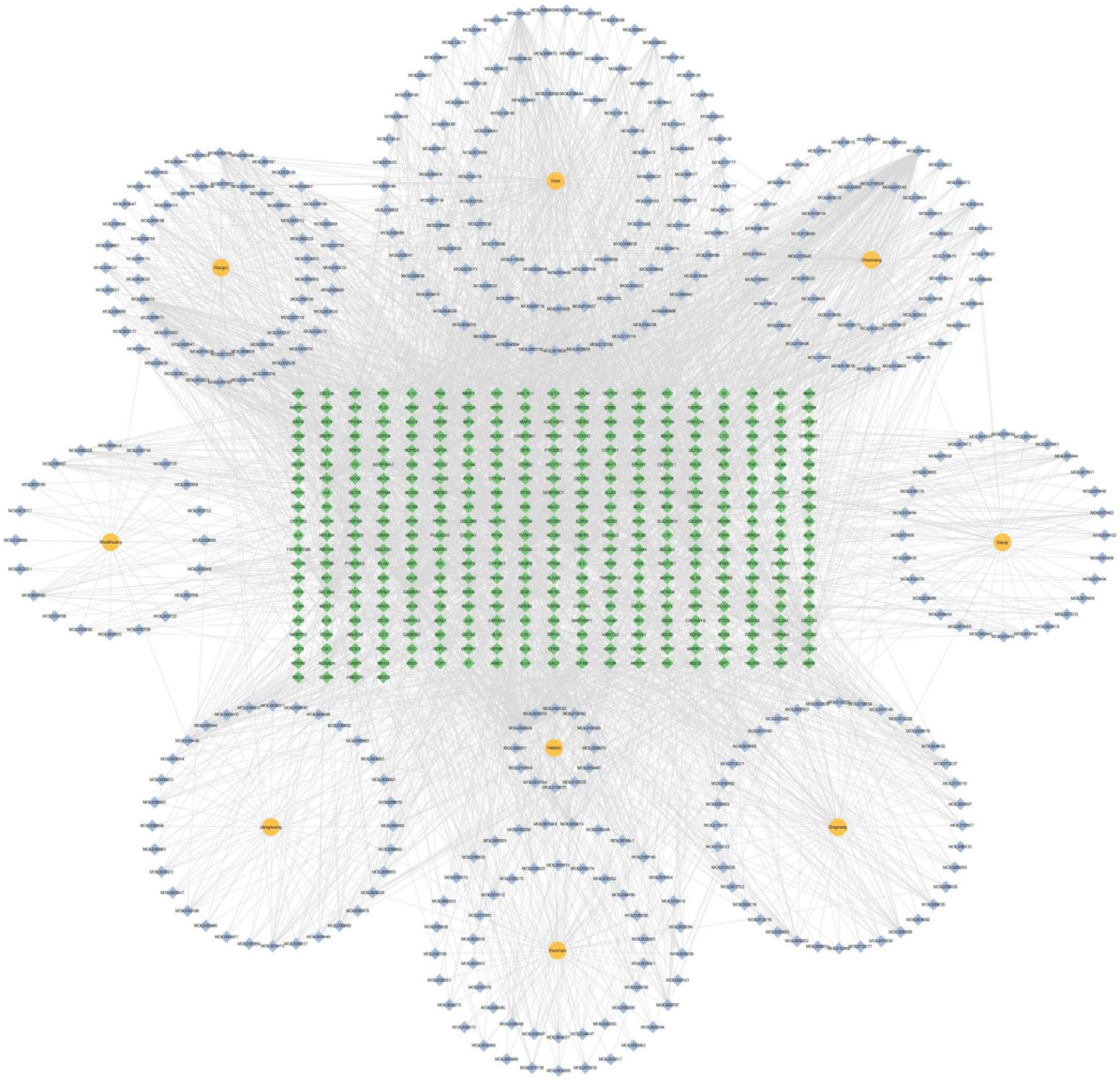

Fig. 1. Herb-Active Component-Target Network.

Molecular docking

Molecular docking showed that cinnamaldehyde forms hydrogen bonds and hydrophobic interactions with key amino acid residues of MAOB, including LYS-271, ILE-264, TYR-393, etc., achieving a binding energy of −7.428 kcal/mol, indicative of strong affinity. Aucubin exhibits favorable affinity and stability with NFKBIA via interactions with residues ARG-56, GLU-64, ASN-175, etc., with a binding energy of −6.902 kcal/mol. These values reflect interaction strength, where lower values signify more stable binding. Binding conformations were visualized using PyMOL, as shown in Fig. 5.

Prognostic evaluation of key markers

Univariate Cox regression analysis identified 21 differentially expressed target genes significantly associated with overall survival in EC (Fig. 6A and Supplementary File 8). Of these, six prognostic factors showed drug activity and molecular relationships in the TCMSP database. Survival analysis (Fig. 6B) revealed that high expression of MAOB, ECE1, TNFRSF10B, HK2, and GPER1 was significantly associated with lower survival probabilities (p values of 0.018, 0.02, 0.019, 0.0073, and 0.0041, respectively), suggesting these markers may indicate a poor prognosis. Conversely, high expression of NFKBIA was associated with a higher survival probability ($p = 0.045$), indicating it may be linked to a better prognosis. Additionally, clinical characteristic analysis of EC (Fig. 6C) showed NFKBIA expression correlated with age ($p < 0.05$), TNFRSF10B expression with gender ($p < 0.05$), and ECE1 expression with tumor stage and histological grade ($p < 0.05$). Other markers (GPER1, HK2, MAOB) showed no significant correlation with these clinical characteristics ($p > 0.05$). These findings suggest these markers could serve as potential prognostic biomarkers for EC patients, with expression levels of certain

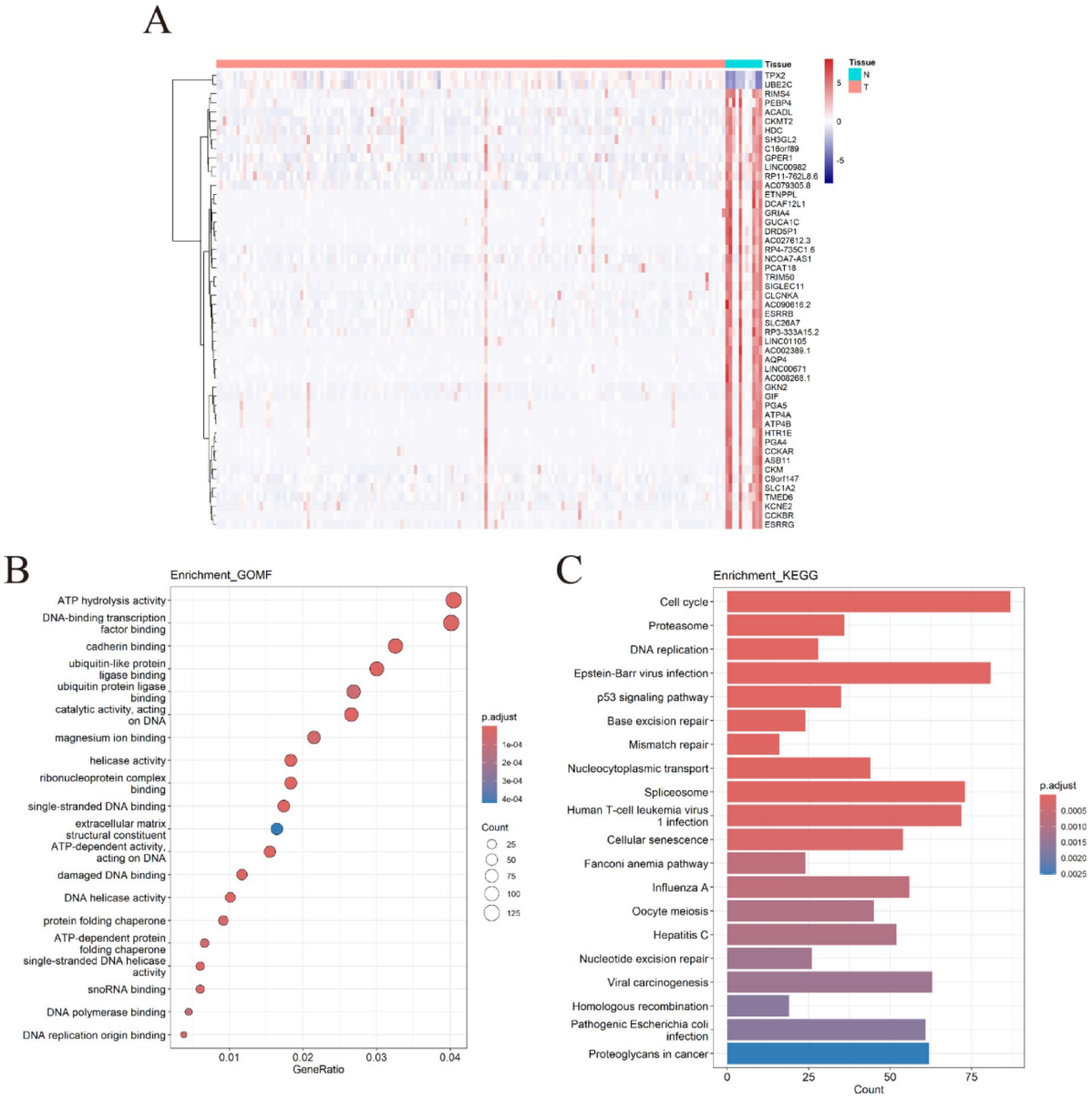

Fig. 2. Differential Expression and Functional Enrichment Analysis. (**A**) Heatmap of differentially expressed genes. (**B**) Molecular function (MF) enrichment. (**C**) KEGG pathway analysis.

markers being influenced by specific clinical characteristics, thereby imparting distinct prognostic significance across different patient groups.

Identification and prediction of active ingredients in DGST

The active components in DGST were identified using UHPLC-MS/MS. Eight classes of chemical compounds were detected, including 394 polyphenolic acids, 338 flavonoids, 269 terpenoids, 178 alkaloids, 137 lignans and coumarins, 32 tannins, 13 quinones, 4 steroids, and 297 compounds of unknown structural types. Representative LC-MS total ion chromatograms were obtained in both positive ionization (ESI+) and negative ionization (ESI−) modes (Fig. 7A and B). Based on database searches and published literature, representative compounds from each herb in DGST were identified and annotated (Table 3). Supplementary File 9 provides the chemical structures and extracted ion chromatograms of all detected compounds.

Expression of key prognostic factors after DGST treatment

Effects of DGST on cell proliferation

To investigate the inhibitory effect of DGST-containing serum on the proliferation of TE-1 and EC-109 cells, we performed CCK-8 assays using four concentration gradients (2%, 5%, 10%, and 20%). The results showed that DGST-containing serum significantly inhibited the proliferation of TE-1 and EC-109 cells in a dose- and time-dependent manner (Fig. 8A). Treatment with 20% DGST-containing serum for 48 h exhibited the most

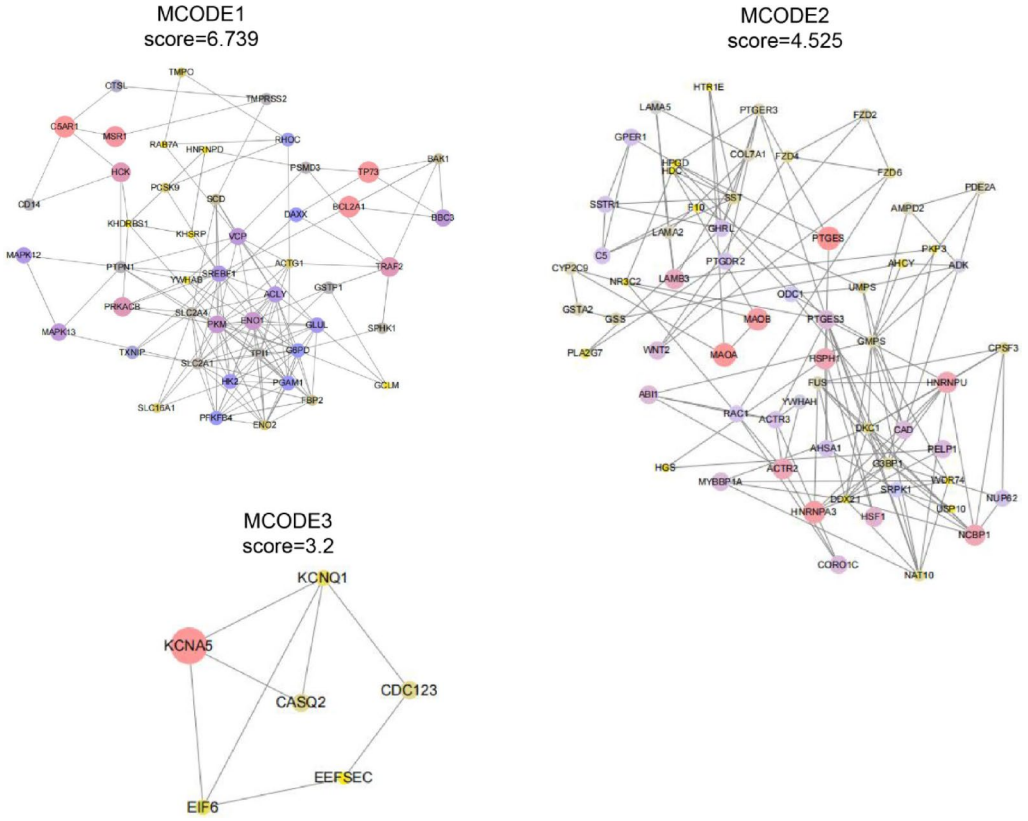

Fig. 3. Network Modules. Two key submodules were identified using the MCODE algorithm in Cytoscape. In the visualization, red nodes represent upregulated genes, blue nodes denote downregulated genes, and the size of each node corresponds to its degree value.

significant inhibitory effect ($p < 0.0001$), and thus we selected this concentration for subsequent experiments. These findings suggest that DGST-containing serum effectively suppresses the proliferation of TE-1 and EC-109 cells.

Effects of DGST on cell apoptosis

Flow cytometry analysis revealed that DGST-containing serum significantly increased the apoptosis rates of EC cells. As shown in Fig. 8B, treatment with 20% DGST-containing serum for 48 h markedly elevated apoptosis rates in both TE-1 and EC-109 cells compared with the control group ($p < 0.001$; $p < 0.01$, respectively). These results indicate that DGST effectively induces apoptosis in EC cells.

Effects of DGST on cell migration and invasion

Transwell assays revealed that DGST-containing serum significantly reduced the migration and invasion capacities of EC cells. Specifically, treatment with 20% DGST-containing serum for 48 h markedly suppressed both migration and invasion capabilities of EC cells. In migration assays, the DGST-treated group exhibited significantly fewer migrated cells compared to the control group ($p < 0.0001$) (Fig. 8C), while in invasion assays, the DGST-treated group showed a pronounced decrease in invaded cells relative to the control ($p < 0.0001$) (Fig. 8D). These results demonstrate that DGST effectively inhibits EC cell migration and invasion, suggesting its potential to suppress tumor metastasis.

Changes in mRNA expression of key prognostic factors

qPCR analysis revealed that treatment with 20% DGST-containing serum significantly altered the mRNA expression levels of key prognostic factors. Specifically, the mRNA levels of *ECE1*, *GPER1*, *HK2*, *MAOB*, and TNFRSF10B were significantly lower in the DGST-treated group than in the control group, whereas *NFKBIA* mRNA levels were markedly higher (Fig. 9E and F). Downregulation of *ECE1*, *GPER1*, *HK2*, *MAOB*, and *TNFRSF10B* correlated with favorable prognosis. Elevated expression of these genes typically associates with tumor invasion, metastasis, and poor prognosis; thus, their reduced expression suggests DGST's potential to improve clinical outcomes. Additionally, upregulation of *NFKBIA* linked to improved prognosis. *NFKBIA* exerts its prognostic benefits by suppressing the NF-κB signaling pathway, thereby attenuating inflammatory responses and cell proliferation, and its elevated expression is generally associated with better clinical outcomes.

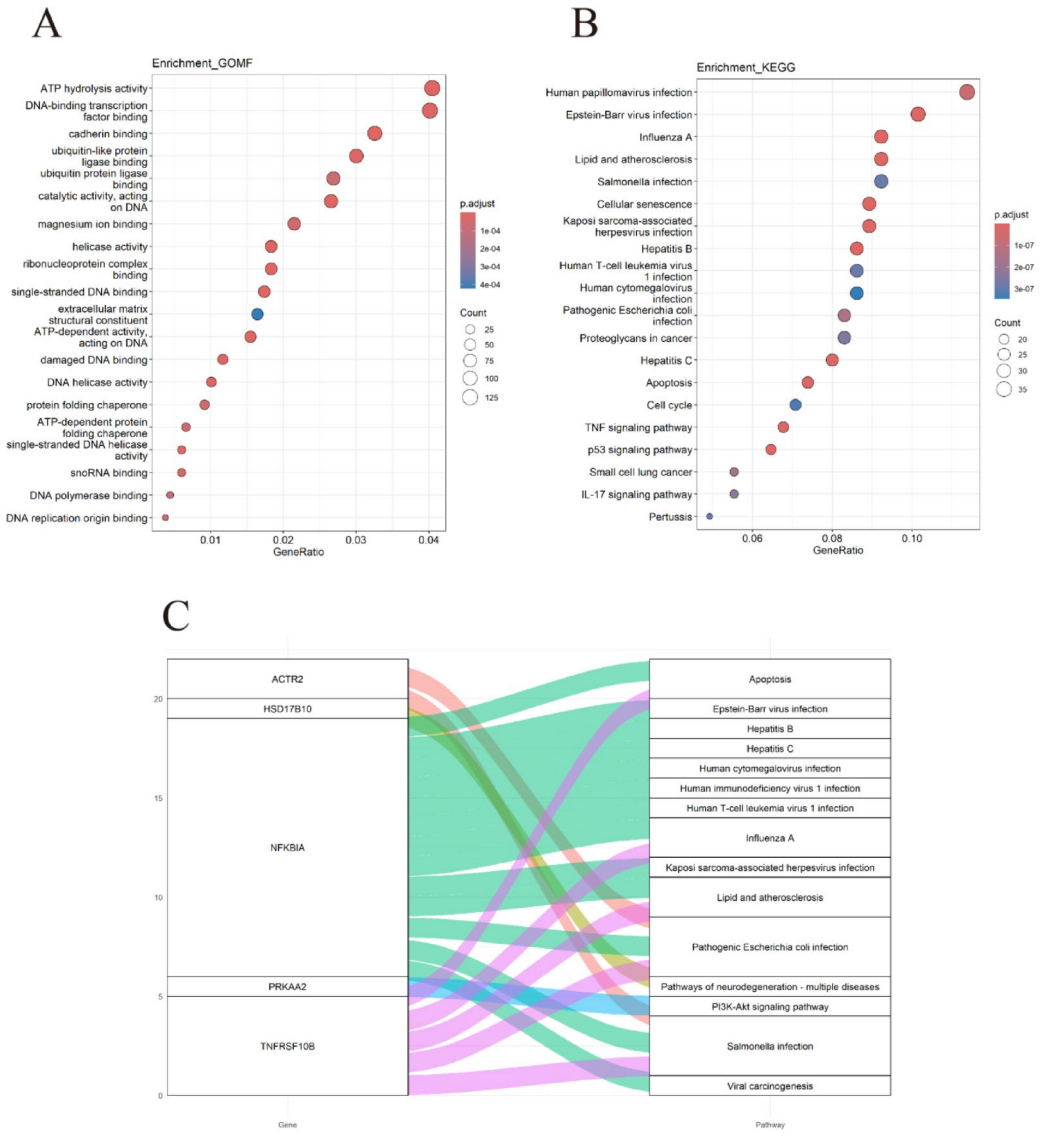

Fig. 4. Molecular function prediction and KEGG pathway analysis of 424 differential target genes. (**A**) Top 20 molecular function pathways ranked by p-value. (**B**) Top 20 KEGG pathways ranked by p-value. (**C**) Network showing the relationships between genes with drug-related pairs in the TCMSP database, molecules, and pathways.

Alterations in the protein levels of critical prognostic factors

To further validate the expression of key prognostic factors in EC following DGST treatment, we performed Western blot analysis. The results corroborated the qPCR findings: as shown in Fig. 9A-D, DGST-containing serum treatment significantly altered the protein expression levels of key prognostic factors (*ECE1*, *GPER1*, *HK2*, *MAOB*, *TNFRSF10B*, and *NFKBIA*). Specifically, compared with the control group, the DGST-treated group (20% serum) exhibited significantly reduced protein levels of *ECE1*, *GPER1*, *HK2*, *MAOB*, and *TNFRSF10B*, alongside a marked increase in *NFKBIA* protein expression.

Discussion

EC is a common malignancy of the digestive tract, characterized by a high incidence rate, significant mortality, and poor prognosis, all of which severely impact patients' quality of life. Studies have demonstrated that factors such as poor dietary habits, smoking, alcohol consumption, obesity, infections, gastroesophageal reflux disease, and genetic predispositions contribute to the onset and progression of EC[15]. Traditional treatment methods for advanced EC stages often exhibit limited efficacy and are frequently accompanied by resistance development. TCM has shown distinct advantages in EC treatment, including boosting patients' immunity, mitigating the adverse effects of radiotherapy and chemotherapy, improving quality of life, and prolonging survival[16]. The development of safe and effective TCM formulations holds great clinical importance.

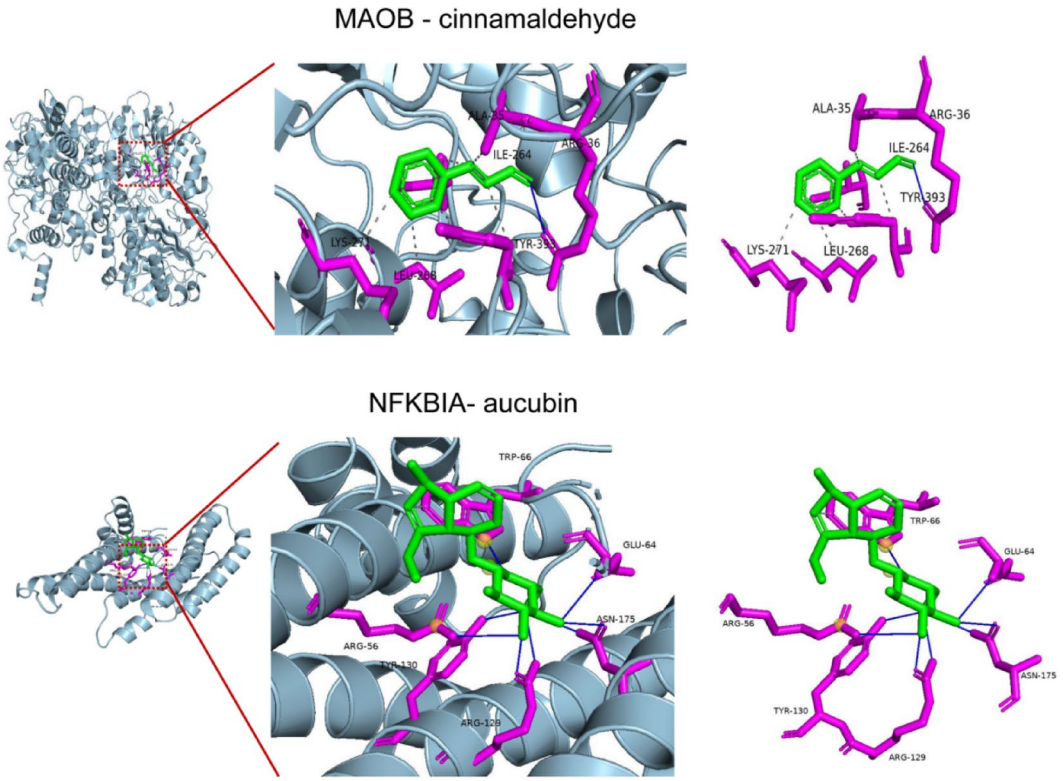

Fig. 5. Molecular Docking. Binding conformations of MAOB with cinnamaldehyde and NFKBIA with aucubin were visualized.

In this study, 424 EC-related differential target genes associated with DGST were identified through network pharmacology. UHPLC-QTOF-MS analysis revealed eight classes of compounds in DGST, including representative compounds such as eugenol[17], aquilarone A[18], ginsenoside Rd[19], cinnamaldehyde[20], β-asarone[21], curcumin[22], and Notoginsenoside R[23], many of which exhibit anti-cancer properties. Prognostic analysis identified 21 genes associated with overall survival, among which six genes—*MAOB*, *NFKBIA*, *TNFRSF10B*, *ECE1*, *HK2*, and *GPER1*— were linked to DGST components. Clinical characteristics analysis showed that *NFKBIA* was associated with age, *TNFRSF10B* was associated with gender, and *ECE1* was associated with tumor stage and histological grade.

The *MAOB* gene encodes an enzyme located on the outer mitochondrial membrane that regulates neurotransmitter levels. Research suggests that *MAOB*may serve as a potential prognostic marker for EC[24], with its expression significantly elevated in hyperplastic samples following EC surgery compared to adjacent non-hyperplastic tissues. This mechanism is likely associated with increased oxidative stress within cells, leading to cellular damage[25]. *TNFRSF10B*, a key member of the tumor necrosis factor receptor superfamily, exhibits heightened expression in various tumor cell types. By binding to TRAIL, it induces apoptosis in tumor cells[26]. Sun et al. developed a prognostic model incorporating SLC25 A5, PPIA, and *TNFRSF10B*to predict correlations with EC prognosis. Their findings revealed significantly higher expression levels of these genes in EC tissues compared to adjacent non-tumor tissues, emphasizing their role in EC progression and the immune microenvironment[27]. ECE1 functions as a potent vasoconstrictor and cell proliferation factor. Elevated ECE1 expression has been observed in multiple cancers, including glioblastoma, prostate cancer, and colon cancer[28]. Wu et al. reported significantly increased ECE1 expression in patients diagnosed with esophageal squamous cell carcinoma, correlating with high tumor invasiveness and serving as a biomarker for poor survival rates and elevated recurrence risks[29]. HK2 is a pivotal enzyme in the initial step of glycolysis and is highly expressed in various cancers. By promoting glycolysis, HK2 provides energy to tumor cells, driving their proliferation and migration. Studies have shown that patients with elevated HK2 expression exhibit significantly reduced five-year survival rates compared to those with lower HK2 levels, supporting the development of HK2-targeted therapies[30,31]. GPER1, a functional oestrogen receptor, mediates immune regulation in cancers such as breast, pancreatic, prostate, and hepatocellular carcinoma[32,33]. By activating signaling pathways, including cAMP/PKA, PI3 K/Akt, and ERK/MAPK, GPER1 influences cell proliferation, differentiation, and apoptosis[34]. The *NFKBIA*gene encodes the IκBα protein, which inhibits NF-κB-mediated expression of pro-proliferative and anti-apoptotic genes, thereby suppressing the growth and survival of EC cells[35,36]. Yu et al. reported that high *NFKBIA*expression in patients with EC negatively correlates with patient survival[37].

In this study, molecular docking analysis revealed that two key target genes (*MAOB* and *NFKBIA*) and their corresponding DGST components (cinnamaldehyde and aucubin) exhibited strong binding affinities. These findings suggest that DGST exerts its effects on EC through a multi-target approach, leveraging the synergistic

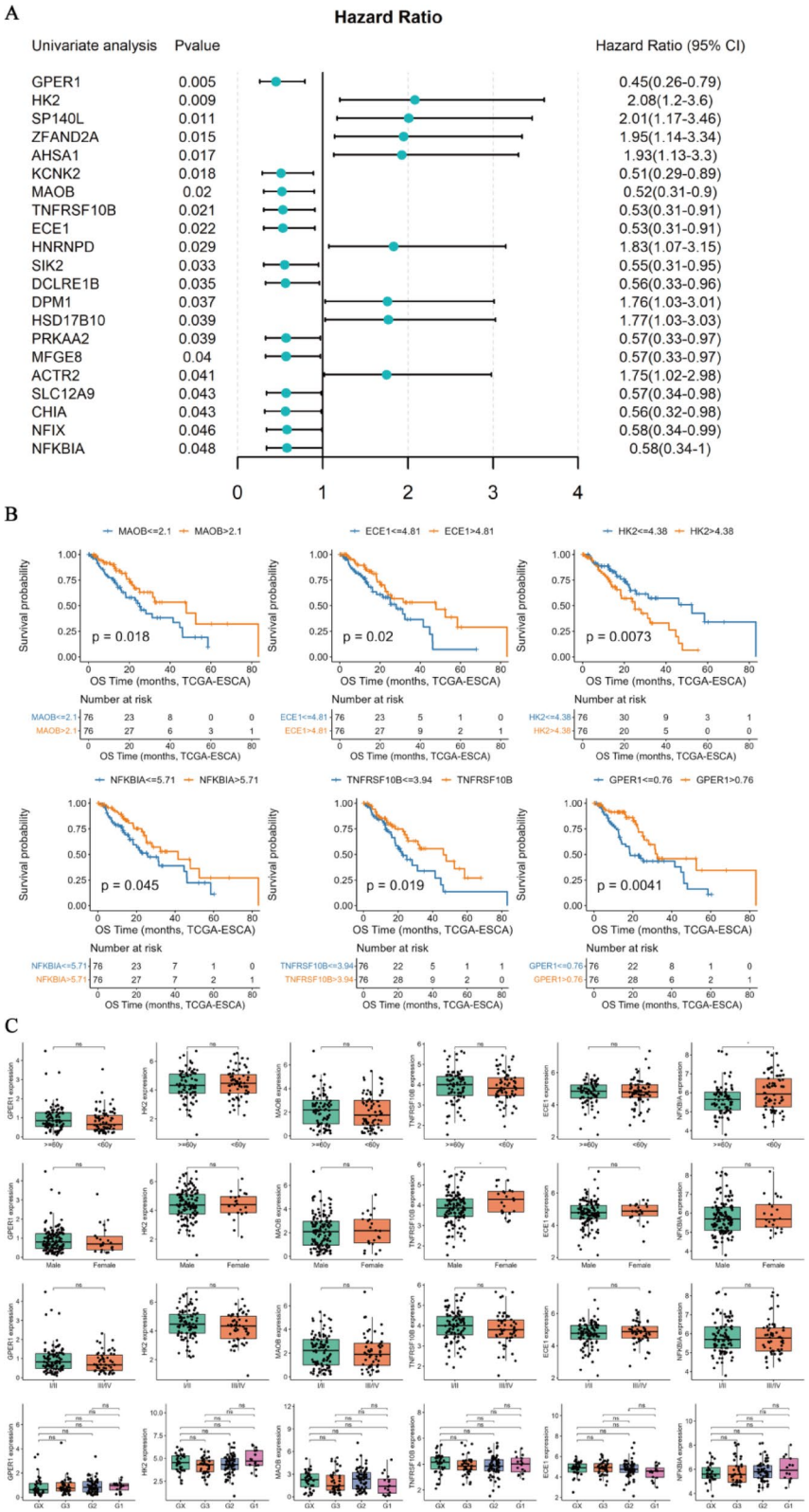

Fig. 6. Survival Analysis of Six Prognostic Factors and Their Relationship with Clinical Characteristics. (**A**) Prognostic Factors Associated with Overall Survival. (**B**) Prognostic Differences of the Six Prognostic Factors. (**C**) Relationship between the Six Prognostic Factors and Clinical Characteristics.

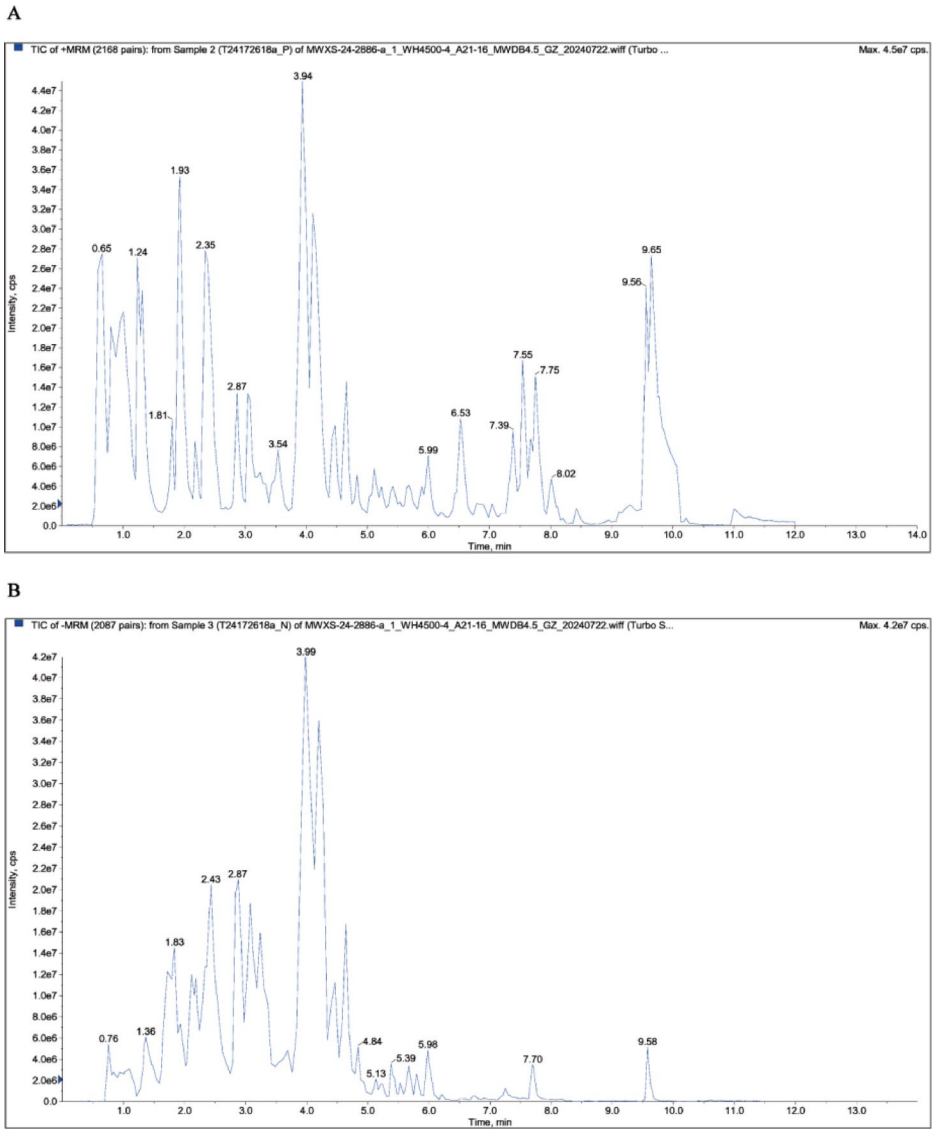

Fig. 7. Active Compounds Identified in DGST. (**A**) DGST analyzed in the ESI + mode. (**B**) DGST analyzed in the ESI − mode.

No	Name	Formula	Class	Intensity	RT (min)
①	Eugenol	C10H12O2	Phenolic acids	15693901.51	6.52
②	2-(2-Phenylethyl)chromone	C17H14O2	Chromone	2749839.562	7.81
③	Ginsenoside Rd	C48H82O18	Triterpene Saponin	40448927.36	6.03
④	Catalpol	C15H22O10	Monoterpenoids	42349.114	0.87
⑤	Cinnamaldehyde	C9H8O	Phenolic acids	262,381	6
⑥	Beta-asarone	C12H16O3	Others	442,179	7.39
⑦	Curcumin	C21H20O6	Phenolic acids	423688.239	7.41
⑧	Notoginsenoside R1	C47H80O18	Triterpene Saponin	4584762.54	4.27
⑨	Phloroglucinol	C6H6O3	Others	1135492.428	2.21

Table 3. Chemical characteristics of bioactive compounds in DGST.

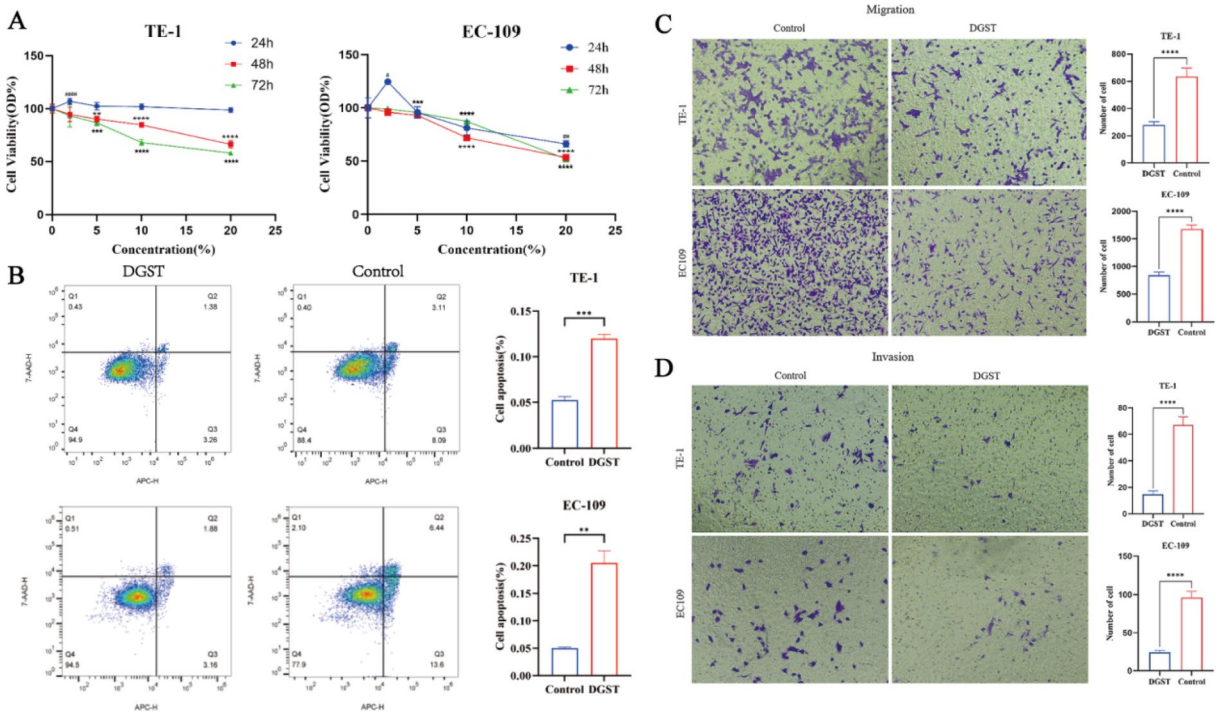

Fig. 8. Effects of DGST Serum on TE-1 and EC-109 Cells. (**A**) Effects of DGST Drug-Containing Serum at Different Concentrations on TE-1 and EC-109 Cell Viability. (**B**) Effects of DGST Drug-Containing Serum on the Apoptosis rate of TE-1 and EC-109 Cells. $^{**}p < 0.01$, $^{***}p < 0.001$ compared to the control group. (**C**) Migration ability of TE-1 and EC-109 cells (×100). (**D**) Invasion ability of TE-1 and EC-109 cells (×100). $^{****}p < 0.0001$ compared to the control group.

actions of various compounds. Additionally, in-vitro experiments demonstrated that DGST significantly suppressed the proliferation, migration, and invasion of esophageal squamous cell carcinoma cell lines TE-1 and EC-109 while promoting apoptosis. PCR and western blot analyses consistently showed that DGST treatment markedly downregulated *MAOB*, *TNFRSF10B*, *ECE1*, *HK2*, and *GPER1* mRNA and protein expression while significantly upregulating *NFKBIA* expression.

These results indicate that DGST significantly regulates key prognostic factors identified through prognostic analysis, suggesting its potential to improve EC prognosis. By targeting these factors, DGST may interfere with tumor proliferation, invasion, metastasis, and metabolism pathways, thereby inhibiting tumor progression and delaying disease deterioration. These findings suggest that DGST components may exert anti-tumor effects through the comprehensive regulation of multiple genes and pathways, highlighting its potential as a complementary therapy to existing treatments for EC, particularly for patients experiencing adverse effects during conventional therapies. This study provides a scientific basis for the development of DGST as a multi-target therapeutic agent for EC.

This study preliminarily validates the bioinformatics analysis results but has certain limitations. For instance, the absence of in vivo experiments limits the translational relevance of the findings. Future studies should prioritize analyzing serum samples from normal and esophageal cancer animal models using mass spectrometry to profile the pharmacokinetics of DGST. Additionally, integrating normal cell cytotoxicity assays will comprehensively evaluate DGST's therapeutic potential, safety, and efficacy. Due to budgetary and time constraints, this study did not validate specific signaling cascades. Moving forward, we will integrate multi-omics technologies to further dissect DGST's roles in key signaling pathways, aiming to elucidate its anti-tumor mechanisms in EC and accelerate clinical translation.

Conclusion

In summary, this study employed network pharmacology and prognostic analysis to explore DGST's potential pharmacological targets and therapeutic mechanisms against EC, and validated these findings through in vitro experiments. The results provide robust evidence supporting DGST's therapeutic application in EC, deepen the understanding of its underlying mechanisms, and establish a theoretical foundation for its future clinical translation and novel drug development.

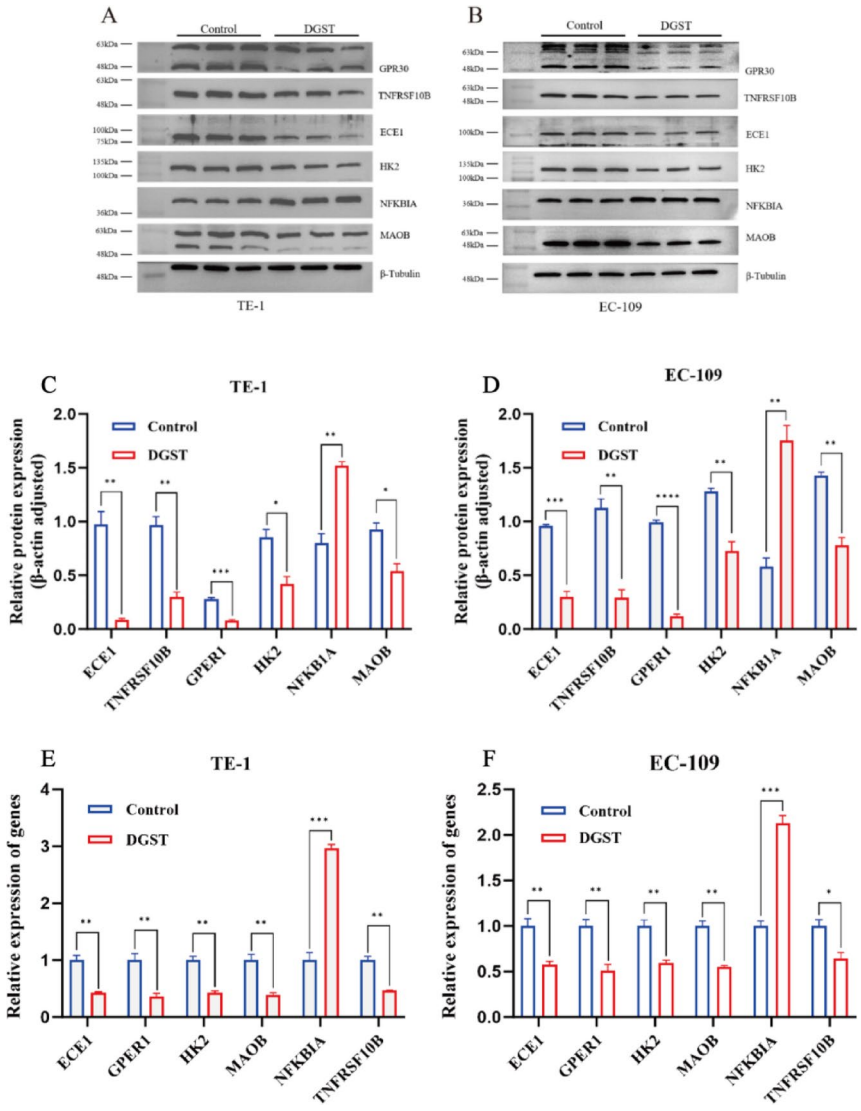

Fig. 9. Effects of DGST on Key Protein and mRNA Expression Levels in TE-1 and EC-109 Cells. (**A**, **C**) Effects of DGST on the protein levels of ECE1, GPER1, HK2, MAOB, TNFRSF10B, and NFKBIA in TE-1 cells. (**B**, **D**) Effects of DGST on the protein levels of ECE1, GPER1, HK2, MAOB, TNFRSF10B, and NFKBIA in EC-109 cells. $^{*}p < 0.05$, $^{**}p < 0.01$, $^{***}p < 0.001$, $^{****}p < 0.0001$ compared to the control group. (**E**, **F**). DGST effects on mRNA expression levels of key prognostic factors in TE-1 and EC-109 cells. $^{*}p < 0.05$, $^{**}p < 0.01$, $^{***}p < 0.001$ compared to the control group.

Data availability

The original contributions presented in the study are included in the article/Additional Files. Further inquiries can be directed to the corresponding authors.

Received: 20 January 2025; Accepted: 2 May 2025
Published online: 28 May 2025

References

1. Morgan, E. et al. The global landscape of esophageal squamous cell carcinoma and esophageal adenocarcinoma incidence and mortality in 2020 and projections to 2040: new estimates from GLOBOCAN 2020. *Gastroenterology* **163**, 649–658e2 (2022).
2. Li, N. et al. Predictions of mortality related to four major cancers in China, 2020 to 2030. *Cancer Commun.* **41**, 404–413 (2021).
3. Wang, Y., Yang, W., Wang, Q. & Zhou, Y. Mechanisms of esophageal cancer metastasis and treatment progress. *Front. Immunol.* **14**, 1206504 (2023).
4. Zhu, H. et al. Esophageal cancer in China: practice and research in the new era. *Intl J. Cancer*. **152**, 1741–1751 (2023).
5. Deboever, N., Jones, C. M., Yamashita, K., Ajani, J. A. & Hofstetter, W. L. Advances in diagnosis and management of cancer of the esophagus. *BMJ* e074962 (2024). https://doi.org/10.1136/bmj-2023-074962
6. Wang, X. et al. Incidence and onset of severe cardiac events after radiotherapy for esophageal Cancer. *J. Thorac. Oncol.* **15**, 1682–1690 (2020).

7. Hong, M. H. et al. A phase II trial of preoperative chemoradiotherapy and pembrolizumab for locally advanced esophageal squamous cell carcinoma (ESCC). *JCO* **37**, 4027–4027 (2019).
8. Cao, L. et al. Traditional Chinese medicine therapy for esophageal cancer: A literature review. *Integr. Cancer Ther.* **20**, 153473542110617 (2021).
9. Chen, X., Deng, L., Jiang, X. & Wu, T. Chinese herbal medicine for oesophageal cancer. *Cochrane Database of Systematic Reviews* (2016). (2016).
10. Zhang, X., Qiu, H., Li, C., Cai, P. & Qi, F. The positive role of traditional Chinese medicine as an adjunctive therapy for cancer. *BST* **15**, 283–298 (2021).
11. Yuling, Z. H. E. N. G. et al. Clinical observation of Dingxiang Guanshitong Hanhua pills alone and its combination with Fugui Guanshitong granules in the treatment of advanced esophageal Cancer. *Chin. Gen. Pract.* **26**, 3765–3771 (2023).
12. Li, X. et al. Network Pharmacology approaches for research of traditional Chinese medicines. *Chin. J. Nat. Med.* **21**, 323–332 (2023).
13. Kanehisa, M., Furumichi, M., Sato, Y., Matsuura, Y. & Ishiguro-Watanabe, M. KEGG: biological systems database as a model of the real world. *Nucleic Acids Res.* **53**, D672–D677 (2025).
14. Kanehisa, M. & Goto, S. KEGG: Kyoto encyclopedia of genes and genomes. *Nucleic Acids Res.* **28**, 27–30 (2000).
15. Arnold, M., Ferlay, J., Van Berge Henegouwen, M. I. & Soerjomataram, I. Global burden of oesophageal and gastric cancer by histology and subsite in 2018. *Gut* **69**, 1564–1571 (2020).
16. Ying, J., Zhang, M., Qiu, X. & Lu, Y. The potential of herb medicines in the treatment of esophageal cancer. *Biomed. Pharmacother.* **103**, 381–390 (2018).
17. Begum, S. N., Ray, A. S. & Rahaman, C. H. A comprehensive and systematic review on potential anticancer activities of Eugenol: from pre-clinical evidence to molecular mechanisms of action. *Phytomedicine* **107**, 154456 (2022).
18. Chen, L., Liu, Y., Li, Y., Yin, W. & Cheng, Y. Anti-Cancer effect of sesquiterpene and triterpenoids from Agarwood of Aquilaria sinensis. *Molecules* **27**, 5350 (2022).
19. Li, H., Han, C., Chen, C., Han, G. & Li, Y. (20S) ginsenoside Rh2-Activated, distinct apoptosis pathways in highly and poorly differentiated human esophageal Cancer cells. *Molecules* **27**, 5602 (2022).
20. Aggarwal, S. et al. Cinnamomum zeylanicum extract and its bioactive component cinnamaldehyde show Anti-Tumor effects via Inhibition of multiple cellular pathways. *Front. Pharmacol.* **13**, 918479 (2022).
21. Hu, Y., Li, Z., Gong, L. & Song, Z. β-Asarone suppresses TGF-β/Smad signaling to reduce the invasive properties in esophageal squamous cancer cells. *Med. Oncol.* **39**, 243 (2022).
22. Wang, W., Li, M., Wang, L., Chen, L. & Goh, B. C. Curcumin in cancer therapy: exploring molecular mechanisms and overcoming clinical challenges. *Cancer Lett.* **570**, 216332 (2023).
23. Li, S. et al. Notoginsenoside R1 induces oxidative stress and modulates LPS induced immune microenvironment of nasopharyngeal carcinoma. *Int. Immunopharmacol.* **113**, 109323 (2022).
24. Zhang, X. et al. A novel mitochondria-related gene signature in esophageal carcinoma: prognostic, immune, and therapeutic features. *Funct. Integr. Genomics.* **23**, 109 (2023).
25. Weng, L. et al. Identification of critical genes and proteins for stent restenosis induced by esophageal benign hyperplasia in esophageal Cancer. *Front. Genet.* **11**, 563954 (2020).
26. Guerrache, A. & Micheau, O. TNF-Related Apoptosis-Inducing ligand: Non-Apoptotic signalling. *Cells* **13**, 521 (2024).
27. Sun, K., Hong, J., Chen, D., Luo, Z. & Li, J. Identification and validation of necroptosis-related prognostic gene signature and tumor immune microenvironment infiltration characterization in esophageal carcinoma. *BMC Gastroenterol.* **22**, 344 (2022).
28. Tapia, J. C. & Niechi, I. Endothelin-converting enzyme-1 in cancer aggressiveness. *Cancer Lett.* **452**, 152–157 (2019).
29. Wu, C. F. et al. High endothelin-converting enzyme-1 expression independently predicts poor survival of patients with esophageal squamous cell carcinoma. *Tumour Biol.* **39**, 101042831772592 (2017).
30. Liu, C. et al. High metabolic rate and stem cell characteristics of esophageal cancer stem-like cells depend on the Hsp27–AKT–HK2 pathway. *Intl J. Cancer.* **145**, 2144–2156 (2019).
31. Liu, X. S. et al. Comprehensive analysis of hexokinase 2 immune infiltrates and m6A related genes in human esophageal carcinoma. *Front. Cell. Dev. Biol.* **9**, 715883 (2021).
32. Ulhaq, Z. S., Soraya, G. V., Milliana, A. & Tse, W. K. F. Association between GPER gene polymorphisms and GPER expression levels with cancer predisposition and progression. *Heliyon* **7**, e06428 (2021).
33. Notas, G., Kampa, M. & Castanas, E. G. Protein-Coupled Estrogen receptor in immune cells and its role in immune-Related diseases. *Front. Endocrinol.* **11**, 579420 (2020).
34. Cimmino, I. et al. Potential mechanisms of bisphenol A (BPA) contributing to human disease. *IJMS* **21**, 5761 (2020).
35. Li, X. & Hu, Y. Attribution of NF-κB activity to CHUK/IKKα-Involved carcinogenesis. *Cancers* **13**, 1411 (2021).
36. Chen, Y. et al. Epigenetically upregulated oncoprotein PLCE1 drives esophageal carcinoma angiogenesis and proliferation via activating the PI-PLCε-NF-κB signaling pathway and VEGF-C/ Bcl-2 expression. *Mol. Cancer.* **18**, 1 (2019).
37. Yu, J. et al. Three-gene immunohistochemical panel predicts progression and unfavorable prognosis in esophageal squamous cell carcinoma. *Hum. Pathol.* **88**, 7–17 (2019).

Acknowledgements

We acknowledge the valuable feedback and constructive suggestions provided by colleagues, which significantly contributed to improving the quality of this manuscript.

Author contributions

Hao Zhang: Data curation, Formal analysis, Investigation, Validation, Visualization, Writing – original draft. Shiqi Wang: Data curation, Formal analysis, Writing – original draft. Xiaoqi Chen: Investigation, Methodology, Project administration, Writing – original draft. Liqi Li: Data curation, Methodology, Validation, Writing – original draft. Yuhong Zheng: Data curation, Validation, Writing – original draft. Yaling Zhang: Investigation, Methodology, Writing – original draft. Xuewen Diao: Investigation, Visualization, Writing – original draft. Yuling Zheng: Formal analysis, Funding acquisition, Project administration, Resources, Supervision, Writing – review & editing. Peiyu Yan: Formal analysis, Funding acquisition, Project administration, Supervision, Writing – review & editing. All authors contributed to the article and approved the submitted version.

Funding

This project was supported by the Science and Technology Development Fund, Macau SAR (Grant No. SKL-QRCM (MUST)-2020-2022, 0011/2021/A), the Henan Provincial Research Project on Traditional Chinese Medicine Science (Grant No. 2023ZYZD05), the National Famous Traditional Chinese Medicine Experts Inheritance Studio Construction Project (Grant No. [2022] 75, issued by the National Administration of Traditional Chinese

Medicine), and the National Famous Traditional Chinese Medicine Inheritance Studio Construction Project (Grant No. [2022] 245, issued by the National Administration of Traditional Chinese Medicine).

Declarations

Ethics approval and consent to participate

All animal experiments were conducted under the supervision of the Ethics Committee of Henan University of Chinese Medicine (Approval number: IACUC-202302040).

Competing interests

The authors declare no competing interests.

Additional information

Supplementary Information The online version contains supplementary material available at https://doi.org/10.1038/s41598-025-00910-w.

Correspondence and requests for materials should be addressed to P.-y.Y. or Y.-l.Z.